Copper–Fluorenephosphonate Cu(PO3-C13H9)×H2O: A Layered Antiferromagnetic Hybrid

Nathalie Hugot, Mélissa Roger, Jean-Michel Rueff, Julien Cardin, Olivier Perez, Vincent Caignaert, Bernard Raveau, Guillaume Rogez, Paul-Alain Jaffres

Copper–Fluorenephosphonate $Cu(PO_3\text{-}C_{13}H_9)\cdot H_2O$: A Layered Antiferromagnetic Hybrid

Nathalie Hugot,[a] Mélissa Roger,[b] Jean-Michel Rueff,*[a] Julien Cardin,[c] Olivier Perez,[a] Vincent Caignaert,[a] Bernard Raveau,[a] Guillaume Rogez,[d] and Paul-Alain Jaffrès[b]

Abstract: A $Cu(PO_3\text{-}C_{13}H_9)\cdot H_2O$ hybrid compound has been synthesized by a hydrothermal method from $Cu(NO_3)_2\cdot 3H_2O$ and 9*H*-fluorene-2-phosphonic acid [$C_{13}H_9PO(OH)_2$]. Its structure was determined by X-ray diffraction performed on a single crystal. The compound crystallizes in the monoclinic centrosymmetric space group $P2_1/a$ [a = 7.4977(5), b = 7.5476(5), c = 22.3702(16) Å, β = 97.794(3)°, V = 1254.23(15) Å^3, Z = 4]. Its lamellar structure consists of alternating organic and inorganic layers. Its organic sub-network is made up of a double layer of fluorene molecules, and its inorganic layer is composed of copper(II) dimers connected to phosphonate groups. In the structure, the neighbouring fluorenyl planes are almost orthogonal to each other, which indicates the absence of π stacking. A study of its magnetic properties, performed on a polycrystalline powder sample, showed antiferromagnetic interactions between the spin carriers without any ordering down to 1.8 K. The interactions between the two copper(II) species within the dimers were evaluated at J = –6.13(5) cm^{-1} with respect to the spin Hamiltonian $\boldsymbol{H} = -J\boldsymbol{S}_{Cu1}\boldsymbol{S}_{Cu2}$. A fluorescence study under excitation at 266 nm showed the disappearance of fluorescence emission in the solid state. This has been attributed to fluorescence quenching by the metallic counterpart.

Introduction

Considerable research effort has been devoted to the synthesis of crystalline hybrid materials over the last decades as a result of their numerous applications, which include, to mention but a few, bio-imaging,[1] gas storage,[2] proton conduction,[3] luminescence,[4] bactericidal properties[5] and other bioapplications.[6] In addition, the properties of these hybrid materials can be tuned by modifying the structure of either the organic part or the inorganic network.[7] In recent years, we have reported on the use of rigid organic precursors,[8] with at least one phosphonic acid functional group to act as a linking group between the organic moiety and the inorganic network,[9] for the synthesis of crystalline hybrid materials. We have previously reported on the development of non-centrosymmetric hybrids[10,11] and thermally stable luminescent materials[12] based on this type of rigid organic precursor. In these studies, the rigidity of the organic moiety results from the presence of a benzene or thiophene ring and is due to the fact that the phosphonic acid functional group is directly bonded to the aromatic ring. However, we have never explored the use of rigid molecules possessing an extended rigid core as an organic platform for the construction of hybrid materials. Fluorene, which was selected as a rigid organic building block for the study reported herein, was previously used after its functionalization with pyridyl moieties to produce Cu^{II}-[13] and Ni^{II}-based[14] metal–organic framework (MOF) materials. Spiro-bis-fluorene functionalized with four carboxylic acid groups has also been used to produce Cu^{II}-based MOF materials.[15] These materials adsorb neutral molecules (e.g., H_2, N_2[15] or I_2[14]) or anionic species (e.g., halides[13]). Finally, 2,7-fluorenonediphosphonic-based materials have very recently been reported. The copper-coordinated 2,7-fluorenonediphosphonic complex also included 2,2′:6′:2″-terpyridine as a ligand.[16] To the best of our knowledge, fluorenephosphonic acid has never been used to produce metal–organic framework materials without an additional ligand. We report herein the synthesis of fluorene-2-phosphonic acid (**2**) and its reaction with copper salts in hydrothermal synthesis to produce the hybrid material $Cu(O_3P\text{-}C_{13}H_9)\cdot H_2O$ (**3**). Its structure was established by single-crystal X-ray diffraction analysis. The magnetic and fluorescent properties of this hybrid material **3** are also reported.

[a] *CRISMAT, CNRS UMR 6508, Ensicaen, 6 bd du Maréchal Juin, 14050 Caen Cedex, France E-mail: jean-michel.rueff@ensicaen.fr http://www-crismat.ensicaen.fr/*
[b] *CEMCA, CNRS UMR 6521, Université de Brest, Université Européenne de Bretagne, IBSAM, 6 Avenue Victor Le Gorgeu, 29238 Brest, France*
[c] *CIMAP, UMR 6252 CNRS, CEA/IRAMIS, Ensicaen, Université de Caen, 6 bd du Maréchal Juin, 14050 Caen Cedex, France*
[d] *IPCMS, UMR UdS-CNRS 7504, 23 rue du Loess, BP 43, 67034 Strasbourg Cedex 2, France*

Results and Discussion

2-Bromofluorene (Scheme 1), which is easily prepared by bromination[17] of fluorene (it is also commercially available), was used as the substrate. The first step consisted of the incorporation of the phosphonate moiety by the nickel-assisted Arbuzov reaction[18] (Tav's method[19]). Accordingly, the expected phosphonate **1** was isolated in 91 % yield (NMR data are presented

in Figure S1 in the Supporting Information). In the last step, the diethyl phosphonate group was hydrolysed in concentrated HCl to produce fluorene-2-phosphonic acid (**2**) in 96 % yield (NMR data are presented in Figure S2).

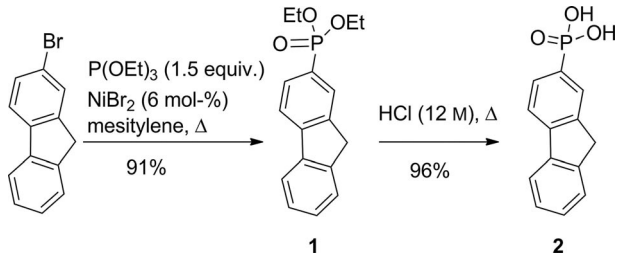

Scheme 1. Synthesis of fluorene-2-phosphonic acid (**2**).

Fluorene-2-phosphonic acid (**2**) was then treated with $Cu(NO_3)_2 \cdot 3H_2O$ under hydrothermal synthesis conditions at 180 °C for 24 h, after which the temperature was slowly decreased to room temperature over 24 h to favour the formation of turquoise-blue crystalline samples of **3**.

TGA was performed on a polycrystalline sample of compound **3** in air to study the weight loss as a function of temperature (Figure 1). The recorded curve can be decomposed into three parts. The compound exhibits thermal stability from room temperature to 156 °C, at which the first plateau is observed. From 156 to 195 °C, a first weight loss of 5.3 wt.-% is observed, which can be attributed to the loss of the single water molecule coordinated to the copper atom (theoretical value: 5.5 wt.-%) leading to a compound of formula $CuPO_3C_{13}H_9$. A second plateau is then observed from 195 to 360 °C, showing the remarkable thermal stability of the dehydrated phosphonate. Powder X-ray diffraction (PXRD) analysis at room temperature after drying of the compound at 200 °C for 2 h in a flow of air revealed a disordered lamellar structure (see Figure SI3 in the Supporting Information). Above 360 °C, a series of weight losses are observed, corresponding to the decomposition of the organic precursor, to give, at 1000 °C, a final weight loss of 53.6 wt.-% [theoretical value 53.8 % for the formula $Cu(PO_3\text{-}C_{13}H_9)\cdot H_2O$], which corresponds to the formation of the purple copper phosphate $Cu_2P_2O_7$. This final compound was unambiguously identified by PXRD (see Figure S4). Elemental analysis (see the Exp. Sect.) confirmed the suggested formula $Cu(PO_3\text{-}C_{13}H_9)\cdot H_2O$ (**3**).

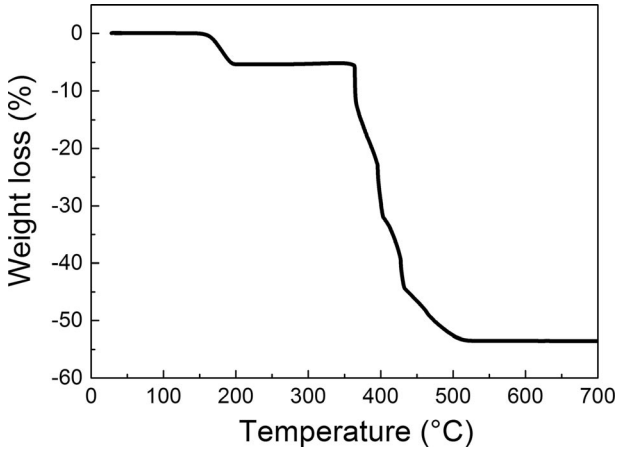

Figure 1. TGA curve of $Cu(PO_3C_{13}H_9)\cdot H_2O$ from 25 to 1000 °C under air recorded at a heating rate of 3 °C min^{-1}.

The crystal data for $Cu(PO_3\text{-}C_{13}H_9)\cdot H_2O$ (**3**; M = 325.74 g mol^{-1}) are presented in Table 1. This compound crystallizes in the space group $P2_1/a$ (no. 14) with the following parameters: a = 7.4977(5), b = 7.5476(5), c = 22.3702(16) Å, β = 97.794(3)°. This sample is monophasic, as shown by its powder X-ray diffraction pattern (see Figure S5 in the Supporting Information).

Table 1. Crystal data, intensity measurement and structure refinement for $Cu(PO_3\text{-}C_{13}H_9)\cdot H_2O$ (**3**).

Formula	$Cu(PO_3\text{-}C_{13}H_9)\cdot H_2O$ (**3**)
Emprical formula	$C_{13}H_{11}CuPO_4$
M [g mol^{-1}]	325.74
Crystal system	monoclinic
Space group	$P2_1/a$
T [°C]	18
a [Å]	7.4977(5)
b [Å]	7.5476(5)
c [Å]	22.3702(16)
β [°]	97.794(3)
Z	4
V [$Å^3$]	1253.23(15)
λ [Å]	0.71073
ρ [g cm^{-3}]	1.666
μ [mm^{-1}]	1.872
F(000)	616.0
2θ range [°]	1.838–64.546
Crystal size [mm]	0.333 × 0.322 × 0.076
Reflections collected	29946
Unique reflections	4404
Goodness of fit	1.0389
R_{int}	0.0225
Final R [$I > 2\sigma(I)$]	0.0246
Final R (all data)	0.0294

$Cu(PO_3\text{-}C_{13}H_9)\cdot H_2O$ (**3**) exhibits a layered structure built up of alternating organic and inorganic slices parallel to (001) (Figure 2). Each organic slice consists of a double layer of fluorene molecules that lie parallel to the c axis; van der Waals interactions between the two fluorene layers ensure the cohesion of the structure. The two-dimensional inorganic sub-network $[Cu\text{-}PO_3]_\infty$ is similar to that previously observed in the hydrated alkyl phosphonates $Cu(PO_3\text{-}CH_3)\cdot H_2O$,[20] $Cu(PO_3\text{-}CH_2CH_3)\cdot H_2O$ and $Cu(PO_3\text{-}CH_2CH_2CH_3)\cdot H_2O$.[22] It is constructed of isolated copper(II) $Cu_2O_6(H_2O)_2$ dimeric units interconnected through single PO_3C tetrahedra (Figure 3). Similar topologies have also been observed in layered copper phosphonates based on 4-(3-bromothienyl)phosphonic acid and 5-(2-bromothienyl)phosphonate.[21]

Each dimeric unit consists of two edge-sharing $CuO_3(H_2O)$ pyramids and shares six oxygen apices with four PO_3C groups and has two free apices occupied by H_2O. The Cu–O distances range from 1.9549 to 2.3832 Å, and the O–Cu–O bond angles range from 81.51 to 170.04° (see Tables S1 and S2 in the Supporting Information; the atom labelling is shown in Figure S6). The distance between two oxygen atoms forming the pyramid is 3.0632 Å, and the distance between two copper atoms forming dimers is 3.1020 Å. The PO_3C groups are directed towards the outside of the inorganic slice and maintain the fluorene moiety parallel to the c axis. Unlike the hydrated $Cu(PO_3\text{-}$

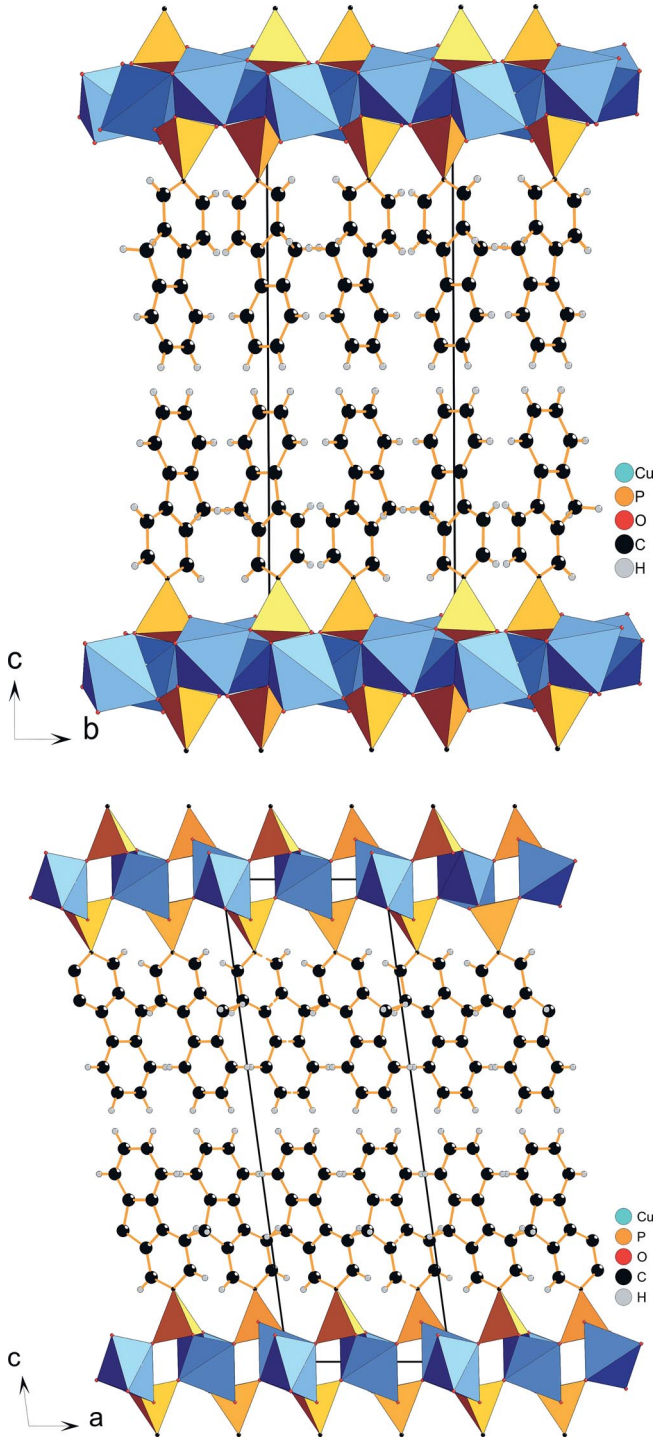

Figure 2. Structural representation of the stacking of organic and inorganic sub-networks of $Cu(PO_3\text{-}C_{13}H_9)\cdot H_2O$ viewed along (a) the *a* axis and (b) the *b* axis.

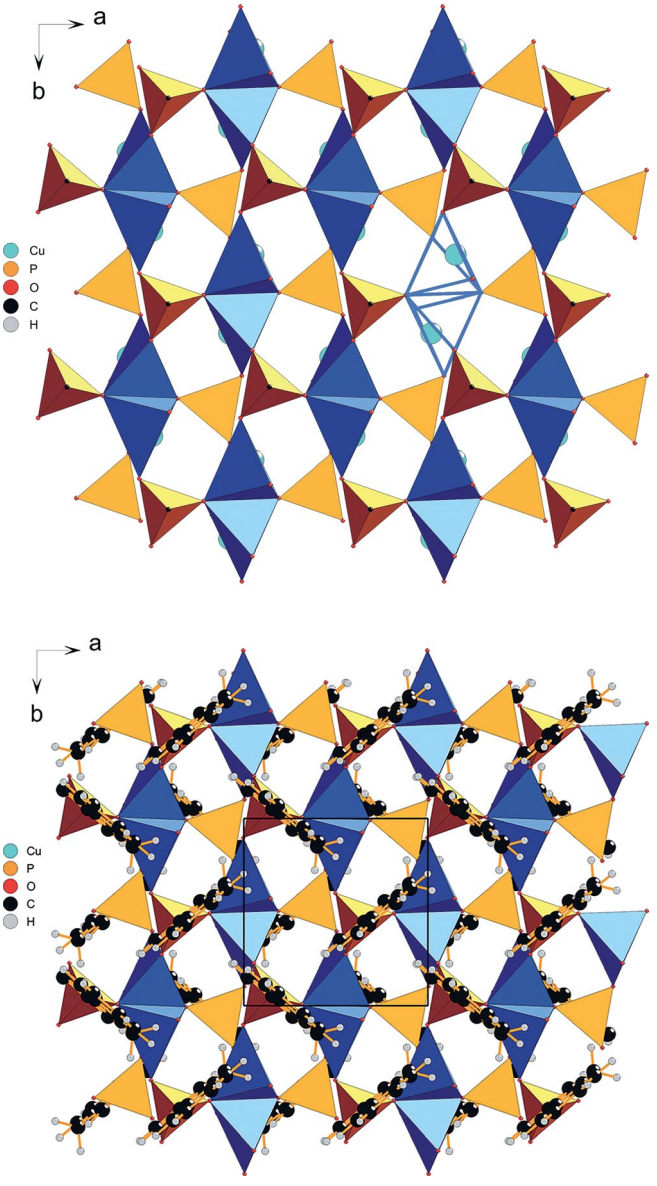

Figure 3. Structural representation of inorganic sub-networks of $Cu(PO_3\text{-}C_{13}H_9)\cdot H_2O$ viewed along the *c* axis: (a) without the fluorene molecules and (b) with the fluorene molecules organized in a herringbone pattern running along the *a* axis.

$CH_2CH_3)\cdot H_2O$ and $Cu(PO_3\text{-}CH_2CH_2CH_3)\cdot H_2O$ copper(II) alkyl phosphonates, in which the alkyl chains are oriented at around 65° with respect to the inorganic plane, the fluorene molecules in $Cu(PO_3\text{-}C_{13}H_9)\cdot H_2O$ are oriented almost perpendicular to the inorganic plane, deviating by about 2.79° from the normal. Finally, in each organic slab the fluorene groups form a double slice and are stacked in a herringbone pattern along the *a* axis (Figure 3, bottom). The parallel orientation of the plane of the aromatic molecules indicates the absence of face-to-face π–π stacking that could have an important impact on the fluorescent properties.

It is worth noting that compound **3** is isostructural with $Cu[PO_3\text{-}(CH_2)_nCH_3]\cdot H_2O$ (n = 0, 1, 2).[20,22] Thus, the rigidity of the fluorenyl moiety, which contrasts with the flexibility of the alkyl chains in $Cu[PO_3\text{-}(CH_2)_nCH_3]\cdot H_2O$, has no effect on the topology of the inorganic network. It can be suggested, as previously observed for rigid precursors,[7] that the rigidity of the organic moiety would more likely modulate the structure of the inorganic part when it is functionalized with at least two functional groups that can be engaged in ion-covalent bonds with the inorganic network.

Next, we assessed the magnetic properties of compound **3**. As already mentioned, the inorganic layer of $Cu(PO_3\text{-}C_{13}H_9)\cdot H_2O$ exhibits a structure similar to those of the hydrated copper(II) alkyl phosphonates of general formula $Cu[PO_3\text{-}(CH_2)_nCH_3]\cdot H_2O$. In $Cu(PO_3\text{-}C_{13}H_9)\cdot H_2O$, the aliphatic chains of $Cu[PO_3\text{-}(CH_2)_nCH_3]\cdot H_2O$ are simply replaced by fluorene molecules acting as spacers. The magnetic interactions in copper alkyl phosphonates have already been described by Le Bideau et al.[23] and Chausson et al.[22] Both groups took into account the structure of the inorganic layers made of isolated copper(II) Cu_2O_8 dimeric units connected through tetrahedral PO_3C phosphonates. The large distances between two isolated dimers cannot allow direct exchange, and the super-exchange path was neglected: these main features logically led to the conclusion that the copper(II) dimeric units are magnetically isolated. Here, similar considerations were adopted to describe the magnetic behaviour of $Cu(PO_3\text{-}C_{13}H_9)\cdot H_2O$.

The variations in the susceptibility χ and χT product as a function of temperature for $Cu(PO_3\text{-}C_{13}H_9)\cdot H_2O$ under a magnetic field of 100 Oe are presented in Figure 4.

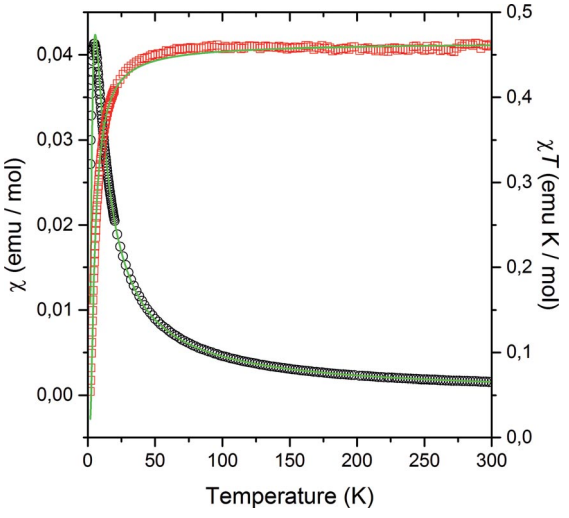

Figure 4. χ (black circles) and χT (red squares) as a function of temperature for compound **3** under a magnetic field of 100 Oe. Full green lines correspond to the best fit of the data (see text).

The data (χ and χT simultaneously) are fitted by Bleaney–Bowers' law[24] by using the following spin Hamiltonian Equation (1) in which all parameters have their usual meaning, and the spin operator $\boldsymbol{S}$ is defined as $\boldsymbol{S} = \boldsymbol{S}_{Cu1} + \boldsymbol{S}_{Cu2}$.

$$\boldsymbol{H} = -J\boldsymbol{S}_{Cu1}\boldsymbol{S}_{Cu2} + g\beta H\boldsymbol{S} \quad (1)$$

The fit leads to the following values: $J = -6.13(5)$ cm^{-1} and $g = 2.23(2)$ with an agreement factor $R = 1 \times 10^{-4}$.[25] These values are in very good agreement with those found by Le Bideau et al.[23]

Fluorescence

Optical experiments (absorbance and photoluminescence) were performed on both compounds **2** and **3**. The measured absorbance decreases as the energy increases (see Figure S7 in the Supporting Information). As no peaks could be observed for either compound it is difficult to assume the involvement of radiative phenomena.

The fluorescence spectra of **2** and **3** were measured in the range 2.0–3.5 eV. The spectrum of fluorenephosphonic acid **2** (measured in methanol solution) shows that the organic ligand is luminescent: one broad peak is observed at 3.04 eV with a full width at half maximum (FWHM) of 0.28 eV. The maximum energy is close to that obtained for similar compounds[26] and can be attributed to π–π^* transitions (see Figure S8 in the Supporting Information). The intensity increases from 3.25 to 3.50 eV, but cannot be explained due to the limitations of the set-up.

In contrast, $Cu(PO_3\text{-}C_{13}H_9)\cdot H_2O$ (**3**) is not fluorescent: it seems that the addition of Cu^{2+} to the organic moiety completely quenches the emission peak. This phenomenon has previously been evidenced for Cu^{2+} complexes featuring fluorophore moieties.[27] Photoinduced electron-transfer mechanisms are usually invoked to explain such a quenching.[28]

Conclusions

Fluorene-2-phosphonic acid [$(HO_2)PO\text{-}C_{13}H_9$, **2**] has been synthesized in two steps from 2-bromofluorene. This compound, which is a rigid arenephosphonic acid due to the presence of the phosphonic acid group directly bonded to the aromatic ring, was used for the preparation of the copper-based hybrid material $Cu(PO_3\text{-}C_{13}H_9)\cdot H_2O$ (**3**). Despite the significant size of the aromatic part (the fluorenyl moiety), the crystal structure of **3** indicates the absence of π stacking within this material. Interestingly, the inorganic layer of material **3** is similar to those observed for copper alkyl phosphonates, which indicates that the rigidity of the organic precursor has no effect on the topology of the inorganic network. This result is likely explained by the fact that the rigid fluorene moiety is functionalized by only one phosphonic acid group. A magnetic study of compound **3** revealed antiferromagnetic properties, and a fluorescence study revealed the complete quenching of the fluorescence emission of **3** [$Cu(PO_3\text{-}C_{13}H_9)\cdot H_2O$] due to the presence of copper atoms. Altogether, these results invite the investigation of materials synthesized from di- or polyfunctionalized fluorenes to evaluate the impact of the rigidity of the fluorene moieties on the topology of the materials and consequently on their properties.

Experimental Section

General: Elemental analyses were recorded with an automatic CHNS-O Thermo-Quest NA 2500 apparatus. The IR spectrum of a turquoise-green polycrystalline sample of **3** (2 wt.-% diluted in KBr) was recorded with a Perkins–Elmer spectrometer working in transmittance mode in the range 450–4000 cm^{-1} at an optical resolution of 4 cm^{-1} and with a Nicolet Nexus (FTIR) spectrometer in ATR mode in the range of 200–4000 cm^{-1} for **1** and **2**. Thermogravimetric analyses were performed with a SETARAM TGA 92 apparatus on a polycrystalline powder sample of $Cu(PO_3\text{-}C_{13}H_9)\cdot H_2O$ with a heating rate of 3 °C min^{-1} from room temperature to 1000 °C under air. Magnetic susceptibility measurements (zero-field-cooled and field-cooled) were performed on a polycrystalline powder by using a Quantum

Design Squid-VSM magnetometer from 2 to 300 K under an applied field of 100 Oe. All compounds were fully characterized by NMR spectroscopy using Bruker AC 300, Avance DRX 400 and Avance DRX 500 spectrometers [^{1}H (500, 400 or 300 MHz), ^{31}P (162 or 121.5 MHz), ^{13}C (125.8 or 75.5 MHz)]. Chemical shifts δ are given in ppm, and coupling constants J are given in Hz. The following abbreviations are used: s singlet, d doublet, t triplet, q quadruplet, m multiplet, dt doublet of triplets. Mass spectra were recorded with a Shimadzu LCMS-2020 spectrometer in electrospray induction (ESI) mode in MeOH. 2-Bromo-9*H*-fluorene was purchased from a commercial source (TCI) and used without further purification. The experimental data for analyses are available in the Supporting Information (see Figures S8 and S9).

Synthesis of the Organic Molecules

Diethyl 9*H*-Fluorene-2-phosphonate (1): $NiBr_2$ (1.34 g, 6.12 mmol, 6 %), 2-bromofluorene (25 g, 102.0 mmol) and mesitylene (30 mL) were placed under nitrogen and heated at 165 °C for 10 min. Triethyl phosphite (22 mL, 127.5 mmol, 1.25 equiv.) was added carefully (the reaction is highly exothermic!) to this solution by a slow and discontinuous dropwise addition. At the end of the addition, the reaction mixture was stirred at 165 °C for a further 5 h. After cooling, the excess triethyl phosphite and mesitylene were removed by distillation under vacuum (ca. 0.1 mbar). The resulting mixture was dissolved in dichloromethane (100 mL) and mixed with water (300 mL) at room temperature overnight. The resulting two layers were separated, and the organic layer was washed with water (2 × 200 mL). The aqueous phase was extracted with dichloromethane (3 × 200 mL). The organic layers were combined, dried with $MgSO_4$ and concentrated under reduced pressure to yield a clear oil. The crude product was purified by silica gel column chromatography (CH_2Cl_2) to yield a white powder. Residual triethyl phosphate (formed as a side-product) was removed by Kugelrohr distillation (100 °C, 10^{-2} Torr) to yield compound **1** in 91 % yield (28.0 g). M.p. 70 °C. R_f (CH_2Cl_2/MeOH, 98:2) = 0.24. ^{1}H NMR ($CDCl_3$, 400 MHz): δ = 1.34 (t, J = 6.8 Hz, 6 H, CH_3), 3.94 (s, 2 H, CH_2), 4.05–4.22 (m, 4 H, CH_2), 7.36 (td, J = 7.2, J = 1.2 Hz, 1 H, H_{ar}), 7.40 (t, J = 6.8 Hz, 1 H, H_{ar}), 7.80–7.87 (m, 3 H, H_{ar}), 8.00 (d, J = 12.8 Hz, 1 H, H_{ar}) ppm. ^{31}P NMR ($CDCl_3$, 162 MHz): δ = 20.4 ppm. ^{13}C NMR ($CDCl_3$, 125 MHz): δ = 16.4 (d, J = 6.8 Hz, CH_3), 36.9 (CH_2), 62.0 (d, J = 5.3 Hz, CH_2), 119.8 (d, J = 16.6 Hz, CH_{ar}), 120.7 (CH_{ar}), 125.2 (CH_{ar}), 125.9 (d, J = 188.7 Hz, C_q), 127.0 (CH_{ar}), 128.0 (CH_{ar}), 128.4 (d, J = 10.5 Hz, CH_{ar}), 130.6 (d, J = 10.5 Hz, CH_{ar}), 140.5 (C_q), 143.1 (d, J = 16.6 Hz, C_q), 143.9 (C_q), 145.8 (C_q) ppm. IR: $\tilde{\nu}$ = 958 (C–O), 1022 (P–O), 1237 (P=O), 2981 (C–H) cm^{-1}. MS (ESI): m/z = 303.05 [M + H]$^+$, 605.25 [2 M – H]$^+$, 630.20 [2 M + H + Na]$^+$.

9*H*-Fluorene-2-phosphonic Acid (2): Compound **1** (25 g, 82.7 mmol) was dissolved in concentrated hydrochloric acid (12 M, 200 mL) and the solution stirred at reflux overnight. The resulting precipitate was filtered and dried under vacuum in a Kugelrohr apparatus (75 °C, 10^{-2} Torr) to yield an off-white powder (1.81 g, 96 %). M.p. >260 °C. ^{1}H NMR (D_2O + K_2CO_3, 400 MHz): δ = 3.97 (s, 2 H, CH_2), 7.37 (t, J = 7.2 Hz, 1 H, H_{ar}), 7.43 (t, J = 7.2 Hz, 1 H, H_{ar}), 7.64 (d, J = 7.2 Hz, 1 H, H_{ar}), 7.75 (dd, J = 8.2, J = 11.6 Hz, 1 H, H_{ar}), 7.87 (dd, J = 8.2, J = 2.4 Hz, 1 H, H_{ar}), 7.91 (t, J = 11.6 Hz, 2 H, H_{ar}) ppm. ^{31}P NMR (D_2O + K_2CO_3, 162 MHz): δ = 12.3 ppm. ^{13}C NMR (D_2O + K_2CO_3, 125 MHz): δ = 39.3 (CH_2), 121.9 (d, J = 13.6 Hz, CH_{ar}), 122.9 (CH_{ar}), 128.2 (CH_{ar}), 129.8 (CH_{ar}), 129.8 (d, J = 9.0 Hz, CH_{ar}), 130.0 (CH_{ar}), 131.8 (d, J = 9.8 Hz, CH_{ar}), 142.4 (d, J = 166.8 Hz, C_q), 143.8 (C_q), 144.1 (d, J = 3.0 Hz, C_q), 145.7 (d, J = 13.6 Hz, C_q), 146.9 (C_q) ppm. MS (ESI): m/z = 247.00 [M + H]$^+$,493.10 [2 M + H]$^+$. IR: $\tilde{\nu}$ = 935 (C–O), 1060 (P–O), 1184 (P=O), 2000–3000 (O–H) cm^{-1}.

Hydrothermal Synthesis of Cu(PO_3-$C_{13}H_9$)·H_2O (3): The inorganic precursor $Cu(NO_3)_2$·$3H_2O$ was commercially (Sigma–Aldrich) obtained, and the organic ligand was synthesized as described previously. Both precursors were used without further purification in the hydrothermal synthesis process. A mixture of 1 equiv. of $Cu(NO_3)_2$·$3H_2O$ (241.60 g mol^{-1}, 0.202 mmol, 0.049 g), 1 equiv. of 9*H*-fluorene-2-phosphonic acid (246.04 g mol^{-1}, 0.203 mmol, 0.05 g), and 1 equiv. of urea (60.06 g/mol, 0.19 mmol, 0.012 g) was dissolved in deionized water (15 mL) and placed in a 20 mL polytetrafluoroethylene (PTFE) liner. The liner was transferred to a Berghof DAB-2 digestive vessel and heated from room temperature to 180 °C in 24 h, maintained at 180 °C for 24 h and then cooled to room temperature over 24 h. The final product obtained as turquoise-blue crystallites was filtered, washed with water and ethanol and dried in air. Yield: 65 %. IR (KBr): $\tilde{\nu}$ = 3279.22 (s), 3002.09 (s), 2911.77 (w), 2353.35 (w), 1917.20 (w), 1818.83 (w), 1725.57 (w), 1610.73 (w), 1570.48 (m), 1410.15 (m), 1397.29 (m), 1303.63 (w), 1281.93 (w), 1240.89 (w), 1205.15 (m), 1192.27 (m), 1173.85 (m), 1111.94 (s), 1074.71 (vs), 1038.35 (vs), 1012.73 (vs), 1000.56 (s), 953.18 (w), 935.34 (m), 908.70 (m), 845.73 (m), 772.31 (m), 752.70 (w), 740.39 (m), 729.84 (s), 680.69 (m), 642.05 (w), 598.44 (s), 582.60 (s), 546.10 (s), 504.25 (w), 478.36 (w) cm^{-1} (see Figure S9 in the Supporting Information). $CuC_{13}H_{11}PO_4$ (325.74): calcd. C 47.93, H 3.40; found C 47.87, H 3.91.

X-ray Diffraction: A suitable single crystal of Cu(PO_3-$C_{13}H_9$)·H_2O was selected, and an X-ray diffraction experiment was performed at room temperature using Mo-K_α radiation produced with a microfocus Incoatec Iμ sealed X-ray tube of a Bruker–Nonius Kappa CCD diffractometer equipped with an Apex2 CCD detector. The Olex2[29] suite was used for structural analysis; a preliminary model was determined by using the "charge flipping" algorithm included in the Superflip program.[30] Refinement was performed by using SHELXL;[31] the analysis of the electronic residue allowed the location of all the missing atomic sites. Harmonic atomic displacement parameters were considered for Cu, P, O and C atoms. Hydrogen atoms were geometrically added. All refinement details are summarized in Table S1 in the Supporting Information. PXRD was performed with an XpertPro diffractometer equipped with a PIXcel detector using Cu-K_α radiation. The data were collected at room temperature from 2.5 to 80° (2θ angular range) in steps of 0.01313°. Further details on the crystal structure investigation may be obtained from Fachinformationszentrum Karlsruhe, 76344 Eggenstein-Leopoldshafen, Germany (fax: +49-7247-808-666; e-mail: crysdata@fiz-karlsruhe.de), on quoting the depository number CSD-430186.

CCDC 430186 (for XX1) contains the supplementary crystallographic data for this paper. These data can be obtained free of charge from The Cambridge Crystallographic Data Centre.

Characterization: Absorbance measurements were performed by using a Perkin–Elmer Lambda 1050 spectrophotometer in transmission mode. Powder samples were deposited on Suprasil® glass slides as optically inactive sample holders. Fluorescence measurements were carried out by using a Lock-in home-built set-up. A 266 nm excitation CryLas CW laser was used as excitation source with a power of 25 mW mm^{-2}. Fluorescence emission collected by lens was dispersed by means of a Horiba Jobin–Yvon TRIAX180 monochromator. The signal was collected at the exit slit of the monochromator with a Hamamatsu R5108 PM tube and recorded with a computer by means of a Stanford Research SRS830 Lock-in amplifier referenced to the 266 nm laser-chopped frequency. Samples for fluorescence measurements were prepared by placing the powder between to Suprasil® glass slides.

Acknowledgments

We thank the Agence Nationale de la Recherche [contract no. ANR-14-CE07-0004-01 (HYMN)] for financial support. The authors also express their grateful acknowledgment for technical support from Sylvie Collin and Fabien Veillon of the CRISMAT laboratory, Sylvie Hernot of the CEMCA laboratory and the Service de RMN, UFR Sciences et Techniques, Université de Bretagne Occidentale, Brest.

Keywords: Fused-ring systems · Organic–inorganic hybrid composites · Phosphorus · Luminescence · Copper

[1] a) A. Foucault-Collet, K. A. Gogick, K. A. White, S. Villette, A. Pallier, G. Collet, C. Kieda, T. Li, S. J. Geib, N. L. Rosi, S. Petoud, *Proc. Natl. Acad. Sci. USA* **2013**, *110*, 17199–17204; b) J. Yu, Y. Cui, C. D. Wu, Y. Yang, B. Chen, G. Qian, *J. Am. Chem. Soc.* **2015**, *137*, 4026–4029.

[2] a) S. R. Miller, E. Alvarez, L. Fradcourt, T. Devic, S. Wuttke, P. S. Wheatley, N. Steunou, C. Bonhomme, C. Gervais, D. Laurencin, R. E. Morris, A. Vimont, M. Daturi, P. Horcajada, C. Serre, *Chem. Commun.* **2013**, *49*, 7773–7775; b) A. C. McKinlay, B. Xiao, D. S. Wragg, P. S. Wheatley, I. L. Megson, R. E. Morris, *J. Am. Chem. Soc.* **2008**, *130*, 10440–10444.

[3] a) R. M. Colodrero, P. Olivera-Pastor, E. R. Losilla, M. A. Aranda, L. Leon-Reina, M. Papadaki, A. C. McKinlay, R. E. Morris, K. D. Demadis, A. Cabeza, *Dalton Trans.* **2012**, *41*, 4045–4051; b) S. Horike, D. Umeyama, S. Kitagawa, *Acc. Chem. Res.* **2013**, *46*, 2376–2384.

[4] a) J. G. Mao, *Coord. Chem. Rev.* **2007**, *251*, 1493–1520; b) B. Mutelet, S. Boudin, O. Perez, J. M. Rueff, C. Labbé, P. A. Jaffrès, *Dalton Trans.* **2015**, *44*, 1186–1192.

[5] M. Berchel, T. Le Gall, C. Denis, S. Le Hir, F. Quentel, C. Elléouet, T. Montier, J. M. Rueff, J. Y. Salaün, J. P. Haelters, P. Lehn, G. B. Hix, P. A. Jaffrès, *New J. Chem.* **2011**, *35*, 1000–1003.

[6] A. C. McKinlay, R. E. Morris, P. Horcajada, G. Férey, R. Gref, P. Couvreur, C. Serre, *Angew. Chem. Int. Ed.* **2010**, *49*, 6260–6266; *Angew. Chem.* **2010**, *122*, 6400.

[7] a) J. M. Rueff, O. Perez, V. Caignaert, G. Hix, M. Berchel, F. Quentel, P. A. Jaffrès, *Inorg. Chem.* **2015**, *54*, 2152–2159; b) J. M. Rueff, M. Poienar, A. Guesdon, C. Martin, A. Maignan, P. A. Jaffrès, *J. Solid State Chem.* **2015**, DOI: 10.1016/j.jssc.2015.09.018.

[8] a) J. M. Rueff, O. Perez, A. Leclaire, H. Couthon-Gourvès, P. A. Jaffrès, *Eur. J. Inorg. Chem.* **2009**, 4870–4876; b) J. M. Rueff, O. Perez, C. Simon, H. Couthon-Gourvès, C. Lorilleux, P. A. Jaffrès, *Cryst. Growth Des.* **2009**, *9*, 4262–4268; c) J. M. Rueff, A. Leclaire, P. A. Jaffrès, *Solid State Sci.* **2009**, *11*, 812–817.

[9] a) J. M. Rueff, V. Caignaert, S. Chausson, A. Leclaire, C. Simon, O. Perez, L. Le Pluart, P. A. Jaffrès, *Eur. J. Inorg. Chem.* **2008**, 4117–4125; b) J. M. Rueff, O. Perez, C. Simon, H. Couthon-Gourvès, C. Lorilleux, P. A. Jaffrès, *Cryst. Growth Des.* **2009**, *9*, 4262–4268.

[10] J. M. Rueff, V. Caignaert, A. Leclaire, C. Simon, J. P. Haelters, P. A. Jaffrès, *CrystEngComm* **2009**, *11*, 556–559.

[11] J. M. Rueff, O. Perez, A. Pautrat, N. Barrier, G. B. Hix, S. Hernot, H. Couthon-Gourvès, P. A. Jaffrès, *Inorg. Chem.* **2012**, *51*, 10251–10261.

[12] J. M. Rueff, N. Barrier, S. Boudin, V. Dorcet, V. Caignaert, P. Boullay, G. B. Hix, P. A. Jaffrès, *Dalton Trans.* **2009**, 10614–10620.

[13] J. P. Ma, Y. Yu, Y. B. Dong, *Chem. Commun.* **2012**, *48*, 2946–2948.

[14] X. M. Zhang, C. W. Zhao, J. P. Ma, Y. Yu, Q. K. Liu, Y. B. Dong, *Chem. Commun.* **2015**, *51*, 839–842.

[15] F. Moreau, N. Audebrand, C. Poriel, V. Moizan-Basleb, J. Ouvry, *J. Mater. Chem.* **2011**, *21*, 18715–18722.

[16] A. Bulut, Y. Zorlu, R. Topkaya, B. Aktaş, S. Doğan, H. Kurt, G. Yücesan, *Dalton Trans.* **2015**, *44*, 12526–12529.

[17] U. J. P. Zimmerman, E. Berliner, *J. Am. Chem. Soc.* **1962**, *84*, 3953–3959.

[18] G. B. Hix, V. Caignaert, J. M. Rueff, L. Le Pluart, J. E. Warren, P. A. Jaffrès, *Cryst. Growth Des.* **2007**, *7*, 208–211.

[19] P. Tavs, *Chem. Ber.* **1970**, *103*, 2428–2436.

[20] a) C. Houttemane, J. C. Boivin, D. J. Thomas, *Acta Crystallogr., Sect. B* **1979**, *35*, 2033–2037; b) Y. Zhang, A. Clearfield, *Inorg. Chem.* **1992**, *31*, 2821–2826.

[21] a) L.-R. Guo, F. Zhu, Y. Chen, Y.-Z. Lia, L.-M. Zheng, *Dalton Trans.* **2009**, 8548–8554; b) W.-X. Nie, S.-S. Bao, D. Zeng, L.-R. Guo, L.-M. Zheng, *Chem. Commun.* **2014**, *50*, 10622–10625.

[22] S. Chausson, J. M. Rueff, M. B. Lepetit, O. Perez, R. Retoux, C. Simon, L. Le Pluart, P. A. Jaffrès, *Eur. J. Inorg. Chem.* **2012**, 2193–2202.

[23] J. Le Bideau, C. Payen, P. Palvadeau, B. Bujoli, *Inorg. Chem.* **1994**, *33*, 4885–4890.

[24] B. Bleaney, K. D. Bowers, *Proc. R. Soc. London, Ser. A* **1952**, *214*, 451–465.

[25] $$R = \frac{\Sigma(\chi_{exp} - \chi_{calcd.})^2}{\Sigma\chi_{exp}^2}.$$

[26] X. H. Zhou, L. Li, A. Li, T. Yang, W. Huang, *Inorg. Chim. Acta* **2014**, *413*, 38–44.

[27] Z. C. Liu, Z. Y. Yang, T. R. Li, B. D. Wang, Y. Li, D. D. Qin, M. F. Wang, M. H. Yan, *Dalton Trans.* **2011**, *40*, 9370–9373.

[28] R. Krämer, *Angew. Chem. Int. Ed.* **1998**, *37*, 772–773; *Angew. Chem.* **1998**, *110*, 804.

[29] O. V. Dolomanov, L. J. Bourhis, R. J. Gildea, J. A. K. Howard, H. Puschmann, *J. Appl. Crystallogr.* **2009**, *42*, 339–341.

[30] a) L. Palatinus, G. Chapuis, *J. Appl. Crystallogr.* **2007**, *40*, 786–790; b) L. Palatinus, A. van der Lee, *J. Appl. Crystallogr.* **2008**, *41*, 975–984; c) L. Palatinus, S. J. Prathapa, S. van Smaalen, *J. Appl. Crystallogr.* **2012**, *45*, 575–580.

[31] G. M. Sheldrick, *Acta Crystallogr., Sect. A* **2008**, *64*, 112–122.